Reports

Wind Tunnel Simulations of Light and Dark Streaks on Mars

Abstract. *Wind tunnel experiments have revealed a characteristic flow field pattern over raised-rim craters which causes distinctive zones of aeolian erosion and deposition. Comparisons of the results with Mariner 9 images of Mars show that some crater-associated dark zones result from wind erosion and that some crater-associated light streaks are depositional.*

It has long been suspected that aeolian, or wind-related, processes occur on Mars, and the suspicion has been confirmed by the results of the Mariner 9 mission (*1*). Both depositional and erosional features have been identified, including dune fields (*2*), "pedestal" craters (*3*), and laminated terrain (*4*). Light and dark streaks, generally associated with craters, are the most abundant aeolian feature identified on the martian surface. During the Mariner 9 mission, many individual craters and streaks were imaged repetitively after the 1971 martian dust storm to observe changes on the surface. Sagan *et al.* (*5*) noted that some dark streaks developed around craters where initially there had been no streaks and that some existing dark streaks significantly changed their shapes and positions; light streaks, however, did not change, and Sagan *et al.* concluded that light streaks are relatively stable. A basic problem is the identification and separation of aeolian depositional streaks from aeolian erosional streaks.

A series of wind tunnel experiments (*6*) is currently in progress to determine criteria for distinguishing erosional from depositional features associated with martian craters and to derive general information on the aeolian regime of Mars. Although all parameters applicable to Mars cannot be satisfied simultaneously in the wind tunnel, a good approximation of the flow field over surface features can be obtained by satisfying appropriate modeling parameters, as discussed by Greeley *et al.* (*7*). This report presents our determination of the aerodynamic flow field over raised-rim craters, the associated zones of erosion and deposition, and comparisons of the results with martian analogs.

Figure 1 presents the results of the wind tunnel experiments, showing the inferred wind flow field over a raised-rim crater and the observed zones of erosion and deposition resulting from the flow field. The flow field was derived from direct observation of the paths of neutral-density helium-filled soap bubbles introduced into the tunnel upwind of the crater and from observations of the motion of sand particles. The flow field appears to be similar to that described for protuberances (with small height-to-diameter ratios) in the planetary boundary layer (*8*) for which a horseshoe vortex wraps around the leading edge of the crater and two trailing vortices stream downwind from the sides of the crater. The tangential component of velocity below the core (near the surface) of both trailing vortices is outward from the crater wake center line, producing a zone of erosion. As the tangential component rises from the surface (Fig. 1), the eroded material is deposited in an area surrounding the crater wake. Downwind from the crater the two axial velocity maxima converge and develop a vortical wind speed on the crater wake center line that is higher than that in the area outside the wake. Thus, areas within the crater wake were preferentially eroded by comparison with surfaces outside the crater wake.

Figure 2, A to C, shows sequential photographs of a raised-rim crater modeled in loose 120-μm quartz sand and placed in the wind tunnel. The crater became ovoid, pointing upwind, and two erosional zones developed downward from the lateral crater flanks. The erosional zones correspond to the trailing components of the horseshoe vortex. Figure 2D shows a small martian crater in Mare Tyrrhenum that is similar to the wind tunnel result. The ovoid outline pointing upwind suggests that the crater rim has been modified by wind erosion on the upwind side and by possible deposition on the downward rim. Although it is unlikely that a direct analogy can be made between the wind tunnel crater modeled entirely in loose sand and the martian crater formed in unknown material (but probably of material more competent than loose sand), it is possible that the windward rim has been sufficiently eroded and the leeward rim modified so as to assume an asymmetric outline. More importantly, the dark streaks downwind from the crater sides have the same morphology and are in the same position in relation to the crater and wind direction as the erosional zones of the wind tunnel experiment, a result which suggests that at least some martian dark streaks are sur-

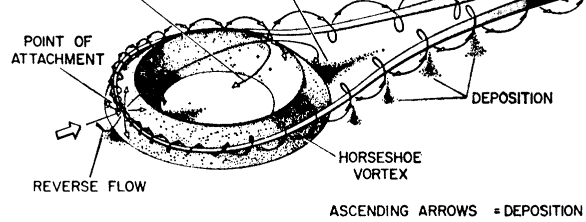

Fig. 1. Proposed flow field over a raised-rim crater, showing the horseshoe vortex and zones of relative erosion and deposition (indicated by the orientation of arrows). Axial velocity maxima (shown as vortex cores) of the trailing vortices converge downwind from the crater, forming a zone of higher surface stress than outside the wake, and hence resulting in erosion. Deposition is continuous parallel to the vortex core.

Scoreboard for Reports: In the past few weeks the editors have received an average of 68 Reports per week and have accepted 12 (17 percent). We plan to accept about 12 reports per week for the next several weeks. In the selection of papers to be published we must deal with several factors: the number of good papers submitted, the number of accepted papers that have not yet been published, the balance of subjects, and length of individual papers.

Authors of Reports published in *Science* find that their results receive good attention from an interdisciplinary audience. Most contributors send us excellent papers that meet high scientific standards. We seek to publish papers on a wide range of subjects, but financial limitations restrict the number of Reports published to about 15 per week. Certain fields are overrepresented. In order to achieve better balance of content, the acceptance rate of items dealing with physical science will be greater than average.

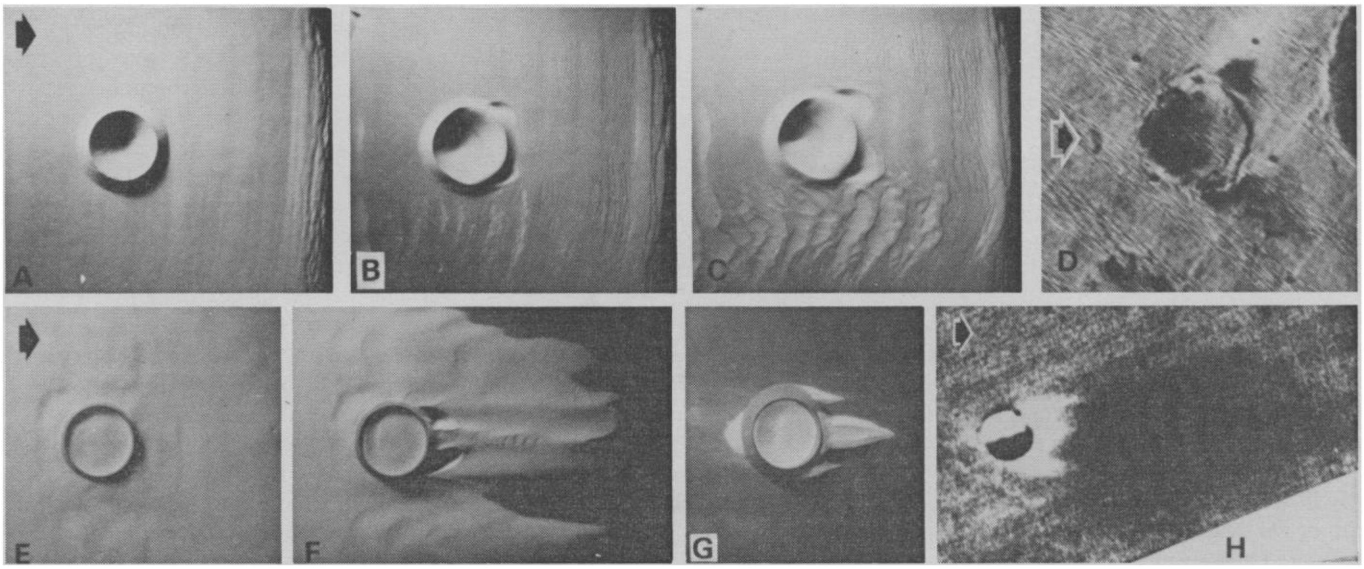

Fig. 2. (A to C) Sequential photographs (light from upper left, wind from left to right as indicated by the arrow) of a 17.8-cm crater modeled in loose sand and placed in the wind tunnel with a wind velocity of about 420 cm/sec. The crater became ovoid in outline, pointing upwind, and developed two erosional depressions corresponding to the trailing components of the horseshoe vortex shown in Fig. 1. (D) Small martian crater in Mare Tyrrhenum showing similar outline and dark zones off the leeward edge of the crater rim that are interpreted to be the result of erosion. (E to G) Sequential photographs of a 17.8-cm crater modeled in solid wood (nondeformable), partly buried by loose sand (E) and subjected to a wind of 850 cm/sec until relatively stable conditions ensued (G) in which the model surface was swept free of loose sand except in zones of relative deposition, shown by the white trilobate pattern and the white patch on the windward rim. (H) A 2-km martian crater in the region northwest of Memnonia showing a similar trilobate pattern in the immediate lee of the crater and a white zone on the windward rim that are interpreted to be aeolian deposits, and a large dark zone in the crater wake area interpreted to have resulted from erosion (Mariner 9 shading-corrected image).

faces that have been swept free of windblown particles. The martian crater in Fig. 2D is typical of many similar craters (each having bilobate dark zones off the leeward rim) observed on Mariner 9 imagery.

Figure 2, E to G, shows sequential photographs of a raised-rim crater modeled in solid wood (and, thus, nondeformable) and partly buried with loose 120-μm sand. Although a higher wind velocity was used than in the experiment of Fig. 2, A to C, similar erosional zones developed (Fig. 2F). Figure 2G shows stable conditions (very slow erosion and deposition compared to the time prior to Fig. 2G) in which the model surface was swept free of particles except in zones of relative deposition. The depositional zones occur in front of the crater, on the floor of the crater, and in a trilobate pattern in the wake of the crater. The trilobate depositional pattern corresponds to the "shadow" zone in the immediate lee of the crater rim, and to the rising tangential component of the trailing vortices.

Figure 2H shows a small (2 km in diameter), bowl-shaped martian crater and associated light and dark surface markings. The white zone on the upwind side of the crater rim and the white trilobate pattern in the lee of the crater have the same shape and relation to the crater as in the wind tunnel experiment and are, therefore, interpreted as deposits of windblown material. The large dark area in the wake of the crater beyond the white trilobate zone corresponds to the zone of maximum vortical wind velocity described above, supporting the hypothesis that at least some martian dark streaks result from erosion. Although the martian crater of Fig. 2H is rather unusual, it is not unique. Several other small craters with similar patterns have been observed on Mariner 9 imagery.

The shapes and positions of the light and dark streaks associated with the martian craters shown in Fig. 2 correspond fairly well with the flow field pattern determined experimentally. Although in wind tunnel simulations, commonly used models are those that are considerably scaled down from the full-size object, there may well be unforeseen problems in applying our results to craters orders of magnitude larger than the wind tunnel models. At this stage of our investigation, however, we are primarily interested in the qualitative determination of the flow field over craters and the resulting zones of erosion and deposition. To test the validity of our wind tunnel results, the erosion and deposition patterns of two craters under natural wind conditions were analyzed. In the first case, a raised-rim crater 6-m in diameter was constructed on a flat field. The crater was examined after each major snowstorm during the winter of 1972 for which there was a single prevailing wind direction. The resulting snowdrift patterns were similar to the pattern of deposition obtained in the wind tunnel, and cleared areas (swept free of snow) were similar to the zones of relative erosion.

The second feature analyzed was Wolf Creek Crater, a natural impact crater 1.2 km in diameter on the Australian desert. It has prominent raised rims and is on flat plains that are partly covered with active aeolian material. A generalized geological sketch map by McCall (*9*) shows the crater and associated sand deposits. Sand has accumulated on the upwind rim, on the crater floor, and in the lee of the crater in an approximately trilobate pattern. Bedrock exposures swept free of aeolian material are shown by McCall to occupy zones between the sand deposits of the trilobate pattern. Although Wolf Creek Crater has not been examined in the field in regard to aeolian processes, the diagram of McCall tends to confirm our wind tunnel determinations of the zones of relative erosion and deposition around raised-rim craters and is on a scale comparable to small martian craters. Thus, the flow field depicted (Fig. 1) appears to be valid for three scales of raised-rim crater—20 cm, 6 m, and 1.2 km—and can be used to explain the origin of the light and dark surface markings associated with the martian craters of Fig. 2. We do not imply, however, that all dark streaks are erosional and that all light streaks are depositional. It has been shown (*2*), for example, that some dark markings appear to be dune fields and hence are the result of deposition. It is likely that some dark and some light markings are erosional and others are depositional. Arvidson's (*10*) analysis of martian light and dark streaks indicates that many long light streaks associated with large craters appear to be erosional. Veverka (*11*) has shown Mariner 9 images on which at least one dark streak appears to be depositional. However, our studies apply to one specific category of crater (small, raised-rim) and each feature must be examined individually in terms of its size, shape, and relation to the surrounding topography in order to assess possible erosion and deposition.

RONALD GREELEY
Physics Department, University of Santa Clara, Santa Clara, California 95053
JAMES D. IVERSEN
Iowa State University, Ames 50010
JAMES B. POLLACK
NASA Ames Research Center, Moffett Field, California 95035
NANCY UDOVICH
University of Santa Clara
BRUCE WHITE
Iowa State University

References and Notes

1. H. Masursky *et al.*, *Science* **175**, 294 (1972).
2. J. A. Cutts and R. S. U. Smith, *J. Geophys. Res.* **78**, 4139 (1973).
3. J. F. McCauley, *ibid.*, p. 4123.
4. B. C. Murray, *Icarus* **17**, 328 (1972).
5. C. Sagan *et al.*, *ibid.*, p. 346.
6. Two wind tunnels are involved: an open-circuit wind tunnel 2.4 m by 0.36 m² at NASA Ames Research Center and an open-circuit environmental wind tunnel 6 m by 1.5 m² at Iowa State University.
7. R. Greeley, J. D. Iversen, J. B. Pollack, N. Udovich, B. White, *Proc. R. Acad. Sci. Lond.*, in press.
8. N. Gregory and W. Walker, *G.B. Aeronaut. Res. Counc. Rep. Mem. No. 2779* (1951), p. 1; R. Sedney, *Am. Inst. Aeronaut. Astronaut. J.* **11**, 782 (1973).
9. G. J. H. McCall, *Ann. N.Y. Acad. Sci.* **123** (No. 2), 970 (1965).
10. R. E. Arvidson, *Icarus*, in press.
11. J. Veverka, personal communication.
12. We thank K. Snetsinger and P. Schultz for reviewing the manuscript. We also thank D. Wong for assistance in the wind tunnel experiments. This work was supported by the Office of Planetology Programs, National Aeronautics and Space Administration.

28 September 1973; revised 26 November 1973

Predictive Simulation of the Subsidence of Venice

Abstract. *Land subsidence at Venice is the result of sediment compaction in the unconsolidated, aquifer-aquitard system that underlies the Venetian Lagoon. Compaction is caused by extensive groundwater withdrawals at the nearby industrial port of Marghera. The total subsidence at Venice for the period from 1930 through 1973 has been about 15 centimeters. Predictive simulations with a calibrated mathematical model were hampered by the sparseness of available data, but, as a first estimate, they suggest that, if withdrawals are kept constant in the future as they have been since 1969, about 3 centimeters of further subsidence can be expected.*

In recent years, worldwide attention has been directed toward Venice, where a collection of environmental problems threatens the existence of this historic and loved city. The problems are threefold. First, there is the periodic flooding of the city caused by the response of the Venetian Lagoon to tides and seiches in the Adriatic Sea; second, there is land subsidence under the influence of heavy groundwater withdrawals in the nearby industrial centers; and third, there is air pollution of industrial origin. In this report we summarize the results of an analysis of the second of these problems: land subsidence in the vicinity of the Venetian Lagoon. For a more complete treatment, the reader is directed to the detailed papers in *Water Resources Research* (*1, 2*).

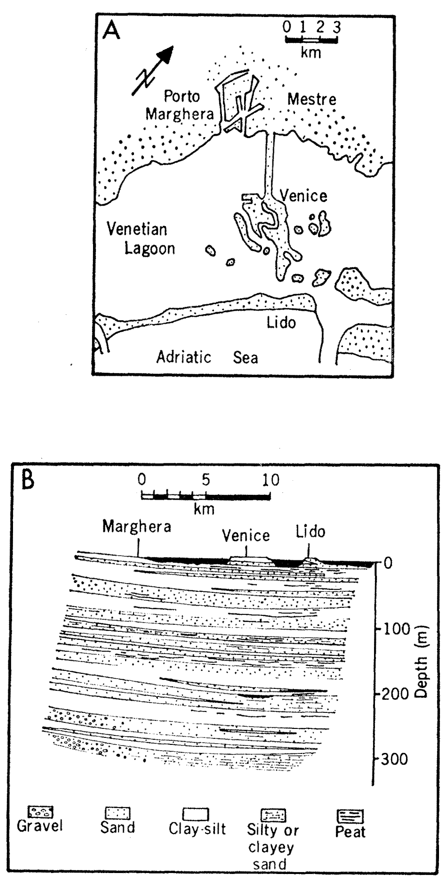

Fig. 1. (A) Location map. (B) Schematic stratigraphic section across the Venetian Lagoon; depth, 0 to 300 m.

The city of Venice occupies a canal-laced group of islands in the Venetian Lagoon, at the northwestern end of the Adriatic Sea (Fig. 1A). The cities of Marghera and Mestre lie on the mainland across the lagoon. The lagoon is shallow, and the sediments underlying it are an extension of those found on the plain that slopes down from the foothills of the Alps toward Venice. The geologic deposits in the upper 1000 m are unconsolidated sands, silts, and clays of Quaternary age.

At the industrial center of Porto Marghera, 7 km from Venice, there are large groundwater withdrawals from about 55 wells that tap five highly permeable aquifers in the upper 300 m. These water-bearing strata are continuous between Marghera and Venice. Extensive industrial pumping started at Porto Marghera in 1930, and by 1969 consumption had reached 460 liter/sec. Since 1969, no new wells have been drilled and pumpage has remained constant. In Venice itself, there is one major well, drilled in 1953, that extracts about 10 liter/sec (*3*).

The total amount of historical subsidence at Venice is not known exactly. It is only during recent years that detailed geodetic surveys have been carried out on a regular basis (1952, 1961, 1969). The observed subsidence during the period from 1952 through 1969 ranges from 9 to 11 cm in Venice and reaches a maximum of 14 cm at the center of the Marghera well field (*4*). These are small values in comparison with the 7- to 8-m subsidence reported for Mexico City and for Long Beach, California, but they are critical in view of the city's setting.

The rate of development of measured subsidence parallels the history of development of the Marghera well field. In light of similar interrelationships at many locations in the world (*5*) and considering the availability of an accepted theory to account for this interrelationship (*1, 6*), we believe that